

Luminescence and Crystal Field Parameters of the $\text{Na}_3[\text{Eu}(\text{ODA})_3] \cdot 7\text{H}_2\text{O}$ Complex in Single Crystalline State

Jun-Gill Kang*, Soo-Kyung Yoon, Youngku Sohn, and Jong-Goo Kim†

Department of Chemistry, Chungnam National University, Taejeon 305-764, Korea

†Korea Atomic Energy Research Institute, Taejeon 302-353, Korea

Received May 17, 1997

Luminescence spectrum of $\text{Na}_3[\text{Eu}(\text{ODA})_3] \cdot 7\text{H}_2\text{O}$ ($\text{ODA} \equiv \text{oxydiacetato}$) was measured at various temperatures. The characteristic band splitting within ${}^5D_0 \rightarrow {}^7F_J$ ($J=1, 2, 3$ and 4) were phenomenologically simulated by using crystal field theory. The set of crystal field parameters reproduces the emission lines in a satisfactory manner with a rms deviation of 21.4 cm^{-1} . It leads the reliable assignment of the luminescence bands and the energy level scheme of 7F_J ($J=1, 2, 3$ and 4) multiplets.

Introduction

Lanthanide ions in trivalent state show very characteristic optical properties of absorption and luminescence spectra. In the UV and visible region, the spectra which are responsible for the $f \rightarrow f$ transitions consist of groups of sharp lines. These transitions are originally forbidden by an electric dipole moment but partially allowed by the crystal field potential.^{1,2} The number of the split lines and their intensities are influenced by the chemical surroundings. When the ion is placed in a specific environment, the spherical symmetry is reduced and the $(2J+1)$ degeneracy is split by the crystal field produced by the ligand. Among lanthanide ions, Eu(III) provides a very useful versatility in the study of the luminescence properties in conjunction with the structural configuration, because of its non-degeneracy of the emitting 5D_0 state.

Lanthanide complexes with tridentate oxydiacetate ligands have drawn considerable attention in spectroscopic studies, since they show chiroptical activity.^{3,4} The structure of $\text{Ln}(\text{ODA})_3^{3-}$ complexes has been well established in terms of the coordination geometry, coordination number and bond distance.⁵ For $\text{Na}_3[\text{Ln}(\text{ODA})_3] \cdot 2\text{NaClO}_4 \cdot 6\text{H}_2\text{O}$,⁵ the crystals form the distorted trigonal prism, in which carboxylic oxygens and ether oxygens lie on twofold axes outside the rectangular faces of the prism and Na^+ ions and water are contained in the layers. Owing to the well-characterized structure, spectroscopic studies of the $\text{Eu}(\text{ODA})_3^{3-}$ complex have been extensively performed in terms of the excitation and emission spectra, the linearly polarized and the circular dichroism absorption spectra, and the magnetic circular dichroism spectrum.⁶⁻¹⁰ Previously, Kirby and Richardson⁶ reported the excitation and emission spectra of $\text{Eu}(\text{ODA})_3^{3-}$ in microcrystalline state. They proposed the assignments for the excitation and emission bands and determined oscillator strengths. Their crystal field parameters set, however, shows a large deviation in the splitting energy gaps.

In this work, the single crystals of $\text{Na}_3[\text{Eu}(\text{ODA})_3] \cdot 7\text{H}_2\text{O}$ were grown by the slow-evaporation method and the luminescence spectra were measured at various temperatures.

The crystal field (CF) parameters were phenomenologically determined by simulating the observed CF splitting with the aid of the CF model. The eigenstates corresponding to the calculated CF levels were also reported.

Experimental

The mother solution was prepared by mixing solutions of europium perchlorate and sodium oxydiacetate to be in the molar 1:3 $\text{Eu(III)}:\text{ODA}$ ratio. The single crystals were grown from the solution at room temperature by the slow-evaporation method. During the evaporation, the pH of the solution was maintained at nearly 5.6.

The TG and DTG spectra were recorded on a Setaram TGA-92 up to 300°C to determine the aqua number of the crystals. The spectra show two distinctive steps due to weight loss in the temperature ranges of $50\text{--}80^\circ\text{C}$ and $150\text{--}190^\circ\text{C}$. From the initial amount of 35.57 mg, the first loss is 3.47 mg and the second loss is 2.17 mg. The weight loss in the low temperature range could be due to the evaporation of solvated water molecules, while the second loss may arise from water molecules coordinated to Eu(III) ions. The quantitative analysis for Na^+ and Eu^{3+} ions was made by the ICP spectrophotometric method on a Jovin-Yvon 50P ICP spectrophotometer. The carbon analysis was also done by an Astro-2001 Analyzer. The wt% of Na^+ , Eu^{3+} and ODA were 10.4, 19.6 and 48, respectively. These quantitative analyses resulted in the calculated formula of the crystals as $\text{Na}_{2.7}\text{Eu}(\text{ODA})_{2.8} \cdot 6.66\text{H}_2\text{O}$. Accordingly, the molecular formula of the single crystals grown in this work is expected as $\text{Na}_3[\text{Eu}(\text{ODA})_3] \cdot 7\text{H}_2\text{O}$. Here, the possibility of the location of sodium perchlorate in the crystals was ruled out since the characteristic 1100 cm^{-1} band of the perchlorate ion was not observed in the IR spectrum.

For optical measurements, a crystal with appropriate size was placed on the cold finger of an Oxford CF-1104 cryostat. Excitation of the crystals was restricted to 395 nm by a conventional Oriel 1000W Xe lamp, passed through a Jovin-Yvon H-20 monochromator. The emission spectrum was measured at a right angle with an ARC 0.5 m Czerny-Turner monochromator equipped with a cooled Hamamatsu R-933-14 PM tube. For the measurement of the excitation spectrum, an Oriel MS257 monochromator replaced the H-

*To whom all correspondence should be addressed.

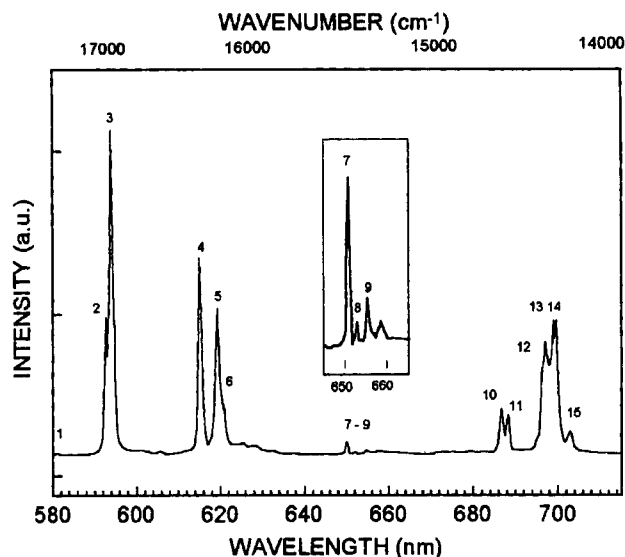


Figure 1. Luminescence spectrum of $\text{Na}_3[\text{Eu}(\text{ODA})_3] \cdot 7\text{H}_2\text{O}$ crystals excited at 395 nm: $T=78.8$ K.

20 monochromator.

Results and Discussion

Luminescence Spectrum. The emission spectrum of the $\text{Na}_3[\text{Eu}(\text{ODA})_3] \cdot 7\text{H}_2\text{O}$ crystals excited at 395 nm, corresponding to the ${}^7F_0 \rightarrow {}^5L_7$ transition, was measured at room temperature, 120 K and 78.8 K. As shown in Figure 1, there is no significant difference between the spectra measured at room temperature and 78.8 K. Only, the band-peak at 699 nm was split to doublet structure at 120 and 78.8 K. Fronczek *et al.*¹¹ suggested that a second-order phase transition in lanthanide complexes might occur between 120 and 5 K. For the $\text{Na}_3[\text{Eu}(\text{ODA})_3] \cdot 7\text{H}_2\text{O}$ crystals, the further line splitting due to the reduction of the site symmetry from D_3 to C_2 did not appear at 78.8 K. The excitation spectrum

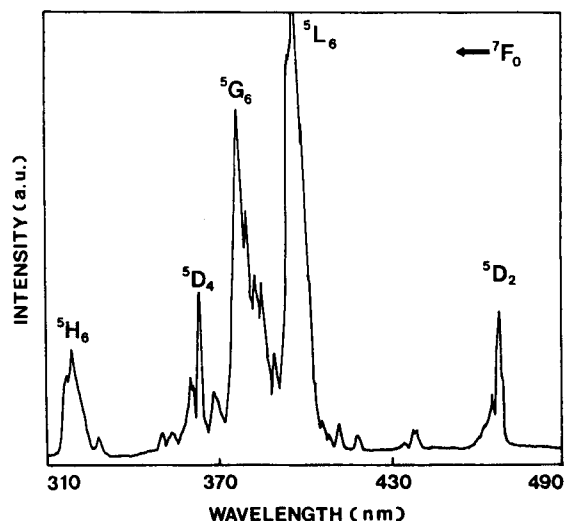


Figure 2. Excitation spectrum of the 618.5 nm emission from $\text{Na}_3[\text{Eu}(\text{ODA})_3] \cdot 7\text{H}_2\text{O}$ crystals measured at room temperature.

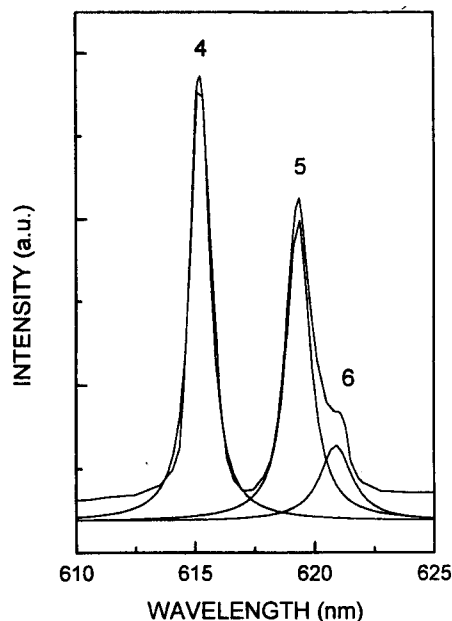


Figure 3. Resolution of a typical emission band by use of Gaussian lineshape function.

for 618.5 nm emission was measured at room temperature. As shown in Figure 2, the 395 nm excitation produces the strongest emission among the observed excitation bands.

For an accurate assignment, the individual lines of the principal bands were deconvoluted in terms of a Gaussian formula. Figure 3 shows a deconvoluted spectrum with expanded scale. The analyzed wavenumbers are listed in Table 1. Under the CF potential within the D_3 symmetry, the $2J+1$ degeneracy will be split into a doublet for $J=1$, a triplet for $J=2$, a quartet for $J=3$, and a sextet for $J=4$. In

Table 1. Experimental and calculated emission lines assigned to the ${}^5D_0 \rightarrow {}^7F_J$ ($J=0, 1, 2, 3$, and 4)

peak no.	$\bar{\nu}_{\text{exp}}$ (cm^{-1})	$\bar{\nu}_{\text{cal}}$ (cm^{-1})	assignment, ${}^5D_0 \rightarrow$
1	17,220		$A_1({}^7F_0)$
2	16,855	16,855	$A_2({}^7F_1)$
3	16,821	16,821	$E({}^7F_1)$
4	16,255	16,255	$E_a({}^7F_2)$
5	16,141	16,142	$A_1({}^7F_2)$
6	16,111	16,111	$E_b({}^7F_2)$
		15,389	$A_2({}^7F_3)$
7	15,375	15,373	$E_a({}^7F_3)$
8	15,323	{ 15,335 15,304 }	$A_{1a}({}^7F_3) + E_b({}^7F_3)$
9	15,267	15,256	$A_{1b}({}^7F_3)$
10	14,560	14,563	$A_{2a}({}^7F_4)$
11	14,524	14,521	$E_a({}^7F_4)$
12	14,343	14,394	$E_b({}^7F_4)$
13	14,306	14,307	$E_c({}^7F_4)$
14	14,290	14,293	$A_{2b}({}^7F_4)$
15	14,225	14,193	$A_1({}^7F_4)$

$\sigma_m = 21.4 \text{ cm}^{-1}$

comparison with the case of the microcrystals of $\text{Na}_3[\text{Eu}(\text{ODA})_3] \cdot 2\text{NaClO}_4 \cdot 6\text{H}_2\text{O}$,⁶ it can be seen that the $\text{Na}_3[\text{Eu}(\text{ODA})_3] \cdot 7\text{H}_2\text{O}$ crystals present the total lifting of the degeneracy in the $^5D_0 \rightarrow ^7F_{1,2,3,4}$ emission bands.

Crystal-Field Simulation. Within the f^n configuration, the CF potential for D_3 symmetry may be written in terms of the spherical tensor operators $C_q^{(k)}$ as¹²

$$V_{CF} = B_0^2 C_0^{(2)} + B_0^4 C_0^{(4)} + B_3^4 (C_{-3}^{(4)} - C_3^{(4)}) + B_0^6 C_0^{(6)} + B_3^6 (C_{-3}^{(6)} - C_3^{(6)}) + B_6^6 (C_{-6}^{(6)} + C_6^{(6)}) \quad (1)$$

where the CF parameters B_q^k are the expansion coefficients, which are empirically determined from the experimental data. Using the Wybourne's formula, the CF matrix elements between two states can be obtained in aid of the sum of the unit tensor, $U_q^{(k)}$ as follows:

$$\begin{aligned} \langle f^n SLJ_z | V_{CF} | f^n \alpha SL'J_z' \rangle \\ = \delta_{SS'} \sum_{k,q} B_q^k \langle f^n \alpha SLJ_z | U_q^{(k)} | f^n \alpha SL'J_z' \rangle = \langle f | | C^{(k)} | | f \rangle \end{aligned} \quad (2)$$

The matrix elements of $U_q^{(k)}$ can be simplified to the reduced matrix elements by the Wigner-Eckart theorem. Here, for the calculation of the CF matrix elements the wavefunctions of the 7F_J states may be constructed in the intermediate coupling scheme since the strong spin-orbit interaction will admix the states with the same J quantum number. The J mixing of the 7F_J states might be mostly expected from the next higher 5D_J states. Among these states, the lowest energy gap can be found between the lowest 7F_0 state and the emitting 5D_0 state. The energy-level structures of these two states can be properly described by the Coulomb interaction, the spin-orbit interaction and the additional interactions due to the linear combinations of radial integrals. Here, the f^6 electronic configuration gives rise to three $^5D\nu$ ($\nu=1, 2$ and 3) terms. The energy matrix of the electrostatic and the spin-orbit interactions and the additional interaction for these $^5D\nu$ terms produced the 5D_3 term the lowest level. Using this term, the secular determinant for the 7F_0 and 5D_0 states was evaluated with energy parameters ($E^1=5.573$, $E^2=26.7$, $E^3=557.4$, $\zeta_{4f}=1326.0$, $\alpha=25.3$, $\beta=-580$ and $\gamma=1156 \text{ cm}^{-1}$), introduced by Carnall *et al.*,¹³ The solution results in the $^5D_0^*$ and $^7F_0^*$ eigenstates in the intermediate coupling scheme: $|^5D_0^*\rangle = 0.9998|^5D_0\rangle + 0.0259|^7F_0\rangle$ and $|^7F_0^*\rangle = -0.0260|^5D_0\rangle + 0.9997|^7F_0\rangle$. This result suggests that in spite of the high degeneracy of the Eu(III) ion, the 7F_J states may be well isolated from other states with the identical J quantum number, so that the matrix elements in eq. (2) can be approximated by the pure 7F_J states.

For a given 7F_J state, the $(2J+1)$ sub-levels can be conveniently divided into classes by introducing the crystal quantum number, μ . The crystal quantum number, μ , is based on the selection rule for the $3j$ symbol, i.e., the CF matrix elements are nonzero if and only if $J_z - J_z' = q$ ($q=0, \pm 3, \pm 6$). The simulation of the CF splittings of the $^7F_{1,2,3,4}$ states was carried out with a combination of the diagonalization and the simplex methods, in which the J mixing between wave functions with different J and J_z values was taken into account. The set of the CF parameters and the barycentres of the luminescence bands were determined by minimizing the root-mean-square (rms) deviation. The fi-

nal values obtained for the B_q^k parameters are $B_0^2=112 (\pm 5) \text{ cm}^{-1}$, $B_0^4=-580 (\pm 5) \text{ cm}^{-1}$, $B_3^4=\mp 810 (\pm 10) \text{ cm}^{-1}$, $B_0^6=760 (\pm 5) \text{ cm}^{-1}$, $B_3^6=\pm 280 (\pm 10) \text{ cm}^{-1}$, and $B_6^6=570 (\pm 10) \text{ cm}^{-1}$. In addition, the barycentres for the 7F_1 , 7F_2 , 7F_3 and 7F_4 states were obtained as 16832, 16162, 15335 and 14385 cm^{-1} , respectively. Starting with the opposite signs of the B_0^4 and B_0^6 values, the refinement of the values yielded a relatively large rms.

The experimental emission lines and the calculated ones are listed in Table 1. The obtained B_q^k parameters produces a very good agreement between the observed and calculated energies except for two lines numbered as 12 and 15. This satisfactory results can lead us to assign the luminescence bands of the $\text{Na}_3[\text{Eu}(\text{ODA})_3] \cdot 7\text{H}_2\text{O}$ accurately. The energies and the eigenstates of the 7F_J ($J=0-4$) were constructed by the set of the CF parameters and the calculated luminescence lines. The obtained eigenstates are listed in Table 2 and the CF splittings are shown in Figure 4. Kirby

Table 2. Energies and major $|J, J_z\rangle$ components calculated by the crystal field effect on the 7F_J multiplets

level	energy	major component
$A_1(^7F_0)$	0	1.00 $ 0, 0\rangle$
$A_2(^7F_1)$	365	1.00 $ 1, 0\rangle$
$E(^7F_1)$	398	1.00 $ 1, \pm 1\rangle$
$E_a(^7F_2)$	965	$-0.03 1, \pm 1\rangle + 0.83 2, \pm 1\rangle + 0.55 2, \mp 2\rangle - 0.02 3, \mp 2\rangle$
$A_1(^7F_2)$	1078	$0.99 2, 0\rangle + 0.12 3, +3\rangle + 0.12 3, -3\rangle$
$E_b(^7F_2)$	1109	$-0.02 1, \pm 1\rangle - 0.54 2, \pm 1\rangle + 0.82 2, \mp 2\rangle - 0.15 3, \pm 1\rangle + 0.04 3, \mp 2\rangle$ $-0.34 3, +3\rangle + 0.87 3, 0\rangle + 0.34 3, -3\rangle + 0.06 $
$A_2(^7F_3)$	1831	$4, +3\rangle + 0.06 4, -3\rangle + 0.07 4, \pm 4\rangle - 0.07 4, \pm 1\rangle$
$E_a(^7F_3)$	1847	$0.03 2, \pm 1\rangle - 0.02 2, \mp 2\rangle + 0.11 3, \pm 1\rangle + 0.99 3, \mp 2\rangle + 0.07 4, \pm 4\rangle - 0.07 4, \pm 1\rangle$
$A_{1a}(^7F_3)$	1885	$0.17 2, 0\rangle + 0.69 3, +3\rangle + 0.69 3, -3\rangle + 0.05 4, +3\rangle - 0.05 4, 0\rangle - 0.05 4, -3\rangle$
$E_b(^7F_3)$	1916	$0.09 2, \pm 1\rangle + 0.13 2, \mp 2\rangle - 0.98 3, \pm 1\rangle + 0.11 3, \mp 2\rangle - 0.05 4, \pm 4\rangle - 0.09 4, \pm 1\rangle + 0.04 4, \mp 2\rangle$
$A_{1b}(^7F_3)$	1964	$0.62 3, +3\rangle + 0.48 3, 0\rangle - 0.62 3, -3\rangle - 0.06 3, +3\rangle + 0.06 3, -3\rangle + 0.63 4, +3\rangle - 0.43 4, 0\rangle - 0.63 4, -3\rangle + 0.12 5, +3\rangle + 0.12 5, -3\rangle$
$A_{2a}(^7F_4)$	2657	$-0.03 3, \mp 2\rangle + 0.10 4, \pm 4\rangle - 0.37 4, \pm 1\rangle - 0.92 4, \mp 2\rangle + 0.09 5, \pm 4\rangle - 0.03 5, \mp 5\rangle - 0.10 3, \mp 2\rangle - 0.75 4, \pm 4\rangle + 0.58 4, \pm 1\rangle - 0.29 4, \mp 2\rangle + 0.05 5, \pm 4\rangle - 0.05 5, \pm 1\rangle - 0.02 5, \mp 2\rangle + 0.03 5, \mp 5\rangle$
$E_c(^7F_4)$	2913	$0.10 3, \pm 1\rangle - 0.64 4, \pm 4\rangle - 0.73 4, \pm 1\rangle + 0.21 4, \mp 2\rangle + 0.05 5, \pm 4\rangle + 0.09 5, \pm 1\rangle - 0.05 5, \mp 2\rangle - 0.05 5, \mp 5\rangle$
$A_{2b}(^7F_4)$	2927	$0.33 3, +3\rangle - 0.04 3, 0\rangle + 0.33 3, -3\rangle + 0.63 4, +3\rangle + 0.63 4, -3\rangle + 0.02 5, +3\rangle - 0.02 5, -3\rangle$
$A_1(^7F_4)$	3027	$0.30 4, +3\rangle + 0.90 4, 0\rangle - 0.30 4, -3\rangle + 0.08 5, +3\rangle + 0.08 5, -3\rangle$

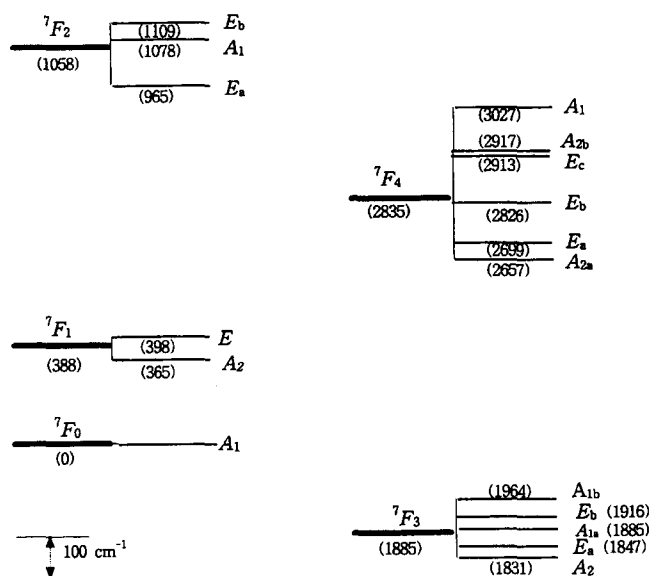


Figure 4. Crystal field splittings of the ${}^7F_{0-4}$ states of $\text{Na}_3[\text{Eu}(\text{ODA})_3] \cdot 7\text{H}_2\text{O}$ crystals, in cm^{-1} , from the simulation of the emission spectrum at 78.8 K.

and Richardson⁶ also reported the calculated energy levels within the 7F_J ($J=0-3$) multiplets. It can be found that their B_q^k parameters give rise to the large discrepancy from the experimental wavenumbers. The better refined set of the CF parameters could be resulted from the fact that single crystals produce more splitting in the luminescence than microcrystallines do.

The eigenfunctions of the 7F_J states determined from the calculated energy scheme may comment on the observed emission intensity. The ${}^5D_0 \rightarrow {}^7F_0$ transition is in principle forbidden but may gain intensity through the J mixing. For the $\text{Na}_3[\text{Eu}(\text{ODA})_3] \cdot 7\text{H}_2\text{O}$ crystals, however, the CF effect does not mix the 7F_0 wavefunction to other ${}^7F_{JM}$ ones, so that the emission band corresponding to the ${}^5D_0 \rightarrow {}^7F_0$ transition appeared only as a trace. Contrary to other ${}^5D_0 \rightarrow {}^7F_J$ transitions, the ${}^5D_0 \rightarrow {}^7F_1$ transition is allowed by the magnetic dipole mechanism. Its intensity is almost independent from the environment and has been strongly observed in most of the Eu(III) complexes. The hypersensitivity of the ${}^5D_0 \rightarrow {}^7F_2$ transition can be discussed with the relative intensity referred to the intensity of the ${}^5D_0 \rightarrow {}^7F_1$ transition. The intensity of the ${}^5D_0 \rightarrow {}^7F_2$ transition is comparable with that of the ${}^5D_0 \rightarrow {}^7F_1$ transition, but somewhat lesser. For isomorphous

$\text{Na}_3[\text{Eu}(\text{DPA})_3] \cdot 9\text{H}_2\text{O}$ (DPA=dipicolinate) crystals, the oscillator-strength ratio of the two bands was found to be about 2.9. The $\text{Na}_3[\text{Eu}(\text{ODA})_3] \cdot 7\text{H}_2\text{O}$ crystals exhibits the strongly enhanced intensity of the ${}^5D_0 \rightarrow {}^7F_2$ transition but not very markedly, compared with the case of $\text{Na}_3[\text{Eu}(\text{DPA})_3] \cdot 9\text{H}_2\text{O}$.¹⁴ The ${}^5D_0 \rightarrow {}^7F_3$ transition is allowed by the electric dipole moment, but always very weak. According to the calculated oscillator strength of the ${}^5D_0 \rightarrow {}^7F_3$ transition,⁶ the ratio of the magnetic-dipole component to the electric-dipole component is about 0.25. The CF effect mixes rarely the 7F_3 wavefunction to the 7F_2 and 7F_4 wavefunctions. Finally, the ${}^5D_0 \rightarrow {}^7F_4$ transition exhibits a moderate intensity, which characterizes somewhat the sensitivity to the environment.

Acknowledgment. This work was supported by the Korean Science and Engineering Foundation (KOSEF 951-0302-019-2).

References

- Judd, B. R. *Phys. Rev.* **1962**, 127, 750.
- Ofelt, G. S. *J. Chem. Phys.* **1962**, 37, 511.
- Sen, A. C.; Chowdhury, M.; Schwartz, R. W. *J. Chem. Soc., Faraday Trans. 2* **1981**, 77, 1293.
- Banerjee, A. K.; Schwartz, R. W.; Chowdhury, M. J. *J. Chem. Soc., Faraday Trans. 2* **1981**, 77, 1635.
- Albertsson, J. *Acta Chem. Scand.* **1968**, 22, 1563; *ibid.*, **1970**, 24, 3527.
- Kirby, A. F.; Richardson, F. S. *J. Phys. Chem.* **1983**, 87, 2557.
- Berry, M. T.; Schwieters, C.; Richardson, F. S. *Chem. Phys.* **1988**, 122, 105.
- Berry, M. T.; Schwieters, C.; Richardson, F. S. *Chem. Phys.* **1988**, 122, 125.
- Görrler-Walrand, C.; Verhoeven, P.; D'Olieslager, J.; Fluyt, L.; Binnemans, K. *J. Chem. Phys.* **1994**, 100, 815.
- Görrler-Walrand, C.; Verhoeven, P.; D'Olieslager, J.; Fluyt, L.; Binnemans, K. *J. Chem. Phys.* **1994**, 101, 7189.
- Fronczek, F. R.; Banerjee, A. K.; Watkins, S. F.; Schwartz, R. W. *Inorg. Chem.* **1981**, 20, 2745.
- Wybourne, B. G. *Spectroscopic Properties of Rare Earths*; Wiley-Interscience: New York, 1965.
- Carnall, W. T.; Fields, P. R.; Rajnak, K. *J. Chem. Phys.* **1968**, 49, 4450.
- will be published elsewhere.